

Measurement of the Docking Time of a DNA Molecule onto a Solid-State Nanopore

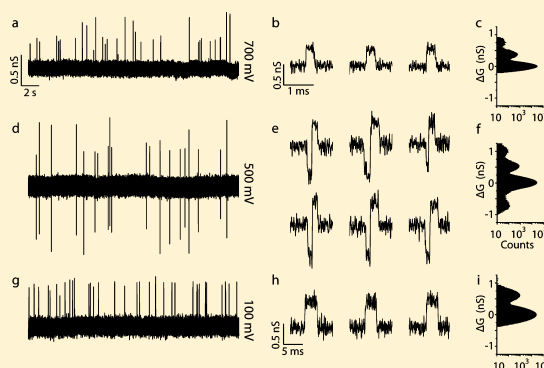
Stefan W. Kowalczyk and Cees Dekker*

Department of Bionanoscience, Kavli Institute of Nanoscience, Delft University of Technology, Lorentzweg 1, 2628 CJ Delft, The Netherlands

Supporting Information

ABSTRACT: We present measurements of the change in ionic conductance due to double-stranded (ds) DNA translocation through small (6 nm diameter) nanopores at low salt (100 mM KCl). At both low (<200 mV) and high (>600 mV) voltages we observe a current enhancement during DNA translocation, similar to earlier reports. Intriguingly, however, in the intermediate voltage range, we observe a new type of composite events, where within each single event the current first decreases and then increases. From the voltage dependence of the magnitude and timing of these current changes, we conclude that the current decrease is caused by the docking of the DNA random coil onto the nanopore. Unexpectedly, we find that the docking time is exponentially dependent on voltage ($t \propto e^{-V/V_0}$). We discuss a physical picture where the docking time is set by the time that a DNA end needs to move from a random location within the DNA coil to the nanopore. Upon entrance of the pore, the current subsequently increases due to enhanced flow of counterions along the DNA. Interestingly, these composite events thus allow to independently measure the actual translocation time as well as the docking time before translocation.

KEYWORDS: Nanopore, access resistance, DNA, translocation



Solid-state nanopores, nanometer-size holes in a thin synthetic membrane are exciting new tools for the detection and manipulation of charged biomolecules.^{1–7} Among many other applications, solid-state nanopores can be used for rapid high-throughput label-free single-molecule detection of small-volume samples of, for example, DNA¹ or DNA–protein⁸ complexes. Much current research is directed toward nanopore sequencing of DNA, both with graphene and biological nanopores (see, for example, ref 9) for the latest developments). The basic working principle is simple: an electric field drives (bio)molecules through the nanopore, thereby inducing characteristic temporary changes in the nanopore ionic current which serve as “fingerprints” of the translocating molecules.

A thorough understanding of the change in ionic conductance when a DNA molecule translocates through a nanopore is evidently of much importance. In particular, temporary current decreases are measured at high salt, whereas the current increases at low salt.^{10–13} This sign change in the current signal could be explained by a simple model,¹⁰ where current decreases at high salt result from a reduced volume for ion flow due to the finite volume occupied by the DNA strand, and current increases at low salt are due to the dominance of an increased density of the counterions (cations) that are brought in by the highly charged DNA backbone. Here, we report a new type of hybrid event, with two distinct current levels—both an increase and decrease level—within each single DNA trans-

location event. As we will show, this provides a new window to separately study the approach of the DNA to the pore and its subsequent translocation through the pore.

First, a single nanopore is fabricated using the focused electron beam of a transmission electron microscope (TEM) in a thin silicon nitride (SiN) membrane. A membrane with a nanopore is then mounted in a microfluidic flow cell and sealed to liquid compartments on both sides of the sample. Subsequent application of an electric voltage (~0.1 V) across the membrane results in an ionic current (~1 nA) through the pore, which is temporarily changed upon passage of a molecule. Measurements are performed in 0.1 M KCl salt solution containing 10 mM Tris-HCl and 1 mM ethylenediaminetetraacetic acid (EDTA) at pH 8.0 at room temperature. All measurements reported in this paper were performed on a single nanopore of 6 nm in diameter, but similar data were measured on three other nanopores of 6 ± 2 nm in diameter. Measurements on larger nanopores (≥ 12 nm in diameter) did not show hybrid events. More detailed information is presented in the Materials and Methods section.

Experimental Results. Figure 1 shows representative current traces for 48.5 kbp double-stranded (ds) DNA translocations in 0.1 M KCl through a 6 nm nanopore

Received: May 7, 2012

Revised: July 3, 2012

Published: July 17, 2012

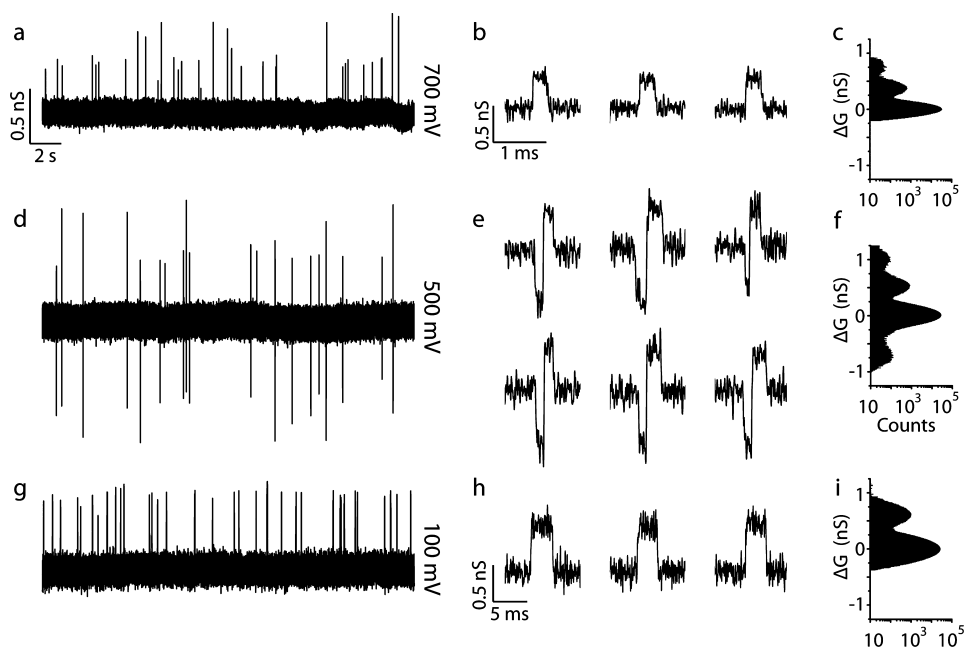


Figure 1. Raw data traces. Spikes appear in the current upon addition of dsDNA to the *cis* side. At 100 and 700 mV the spikes all go in upward direction; that is, current increases (a, e). At 500 mV the spikes seemingly go synchronously both up and down (d). Zooming in on representative individual events, we see that, within single events at 500 mV, the current first decreases and then increases (e). At 100 and 700 mV the events are composed of a single current level; that is, only current increases (b, h). All data were taken at 0.1 M KCl. For display purposes the traces in (b, e) are low-pass filtered at 30 kHz; a, d, and h are filtered at 10 kHz, and g is filtered at 2 kHz. The scale bar in part a also applies to d and g; the scale bar in b also applies to e. Conductance histograms of all events (including 10 ms of baseline before and after an event) measured at respectively 700, 500, and 100 mV bias.

recorded at 100, 500, and 700 mV. Spikes appear in the current upon addition of dsDNA to the *cis* side. At both 100 mV and 700 mV, the spikes all go in the upward direction; that is, the current increases upon DNA translocation; see Figure 1a,g, which is the expected low-salt behavior. Interestingly, at 500 mV, however, the spikes go both up and down (Figure 1d). Zooming in on representative individual events at 500 mV, we see that, within each single event, the current first decreases and then increases (Figure 1e). This happens for a large majority of events (on average for 87% of events in the regime from 200 to 600 mV; the remaining 13% are events where the current only increases). At 100 and 700 mV, by contrast, 100% of the events are composed of a single current increase; see Figure 1b,h.

We first analyze the magnitudes of both the conductance decrease and increase levels $\Delta G \equiv \Delta I/V$ and how these scale with voltage. Figure 1c, f, and i shows the conductance histogram of all events recorded at 700, 500, and 100 mV (obtained from respectively 134, 168, and 185 events, including 10 ms of open-pore conductance before and after each event). We find the characteristic ΔG values by fitting Gaussian distributions to the conductance blockade histograms. Note that typically we find only a peak (or multiple peaks due to folding, see below) at positive values of conductance change, such as for 100 and 700 mV. But at 500 mV, we also find a peak at a negative conductance change, i.e., at $\Delta G = -0.7$ nS in this example.

Figure 2a shows that the voltage dependence of the magnitude of these ΔG changes. The conductance decrease (negative ΔG) strongly increases with voltage. On the other hand, the conductance increases (positive ΔG) are getting smaller with voltage, except for small voltages (<150 mV, where it was previously suggested that counterions at very low fields are condensed on the DNA but at higher fields start to glide

along the DNA and produce an additional current), similar to the behavior reported before for slightly larger pores.¹³

Next we perform an analysis of the relative duration of the times spent at each current level. Each hybrid event is divided into its natural two parts (i.e., current increase and decrease), and we measure the duration t_1 of the first part and that of the second part t_2 (see Figure 3a). A scatter plot is shown in the Supporting Information, see Figure S2. Figure 3b displays t_1 (red dots) and t_2 (black squares) versus voltage on a linear scale. We observe that $t_1 > t_2$ below about 350 mV, while $t_1 < t_2$ above 350 mV. Plotting the same data on a log–log scale (Figure 3b) and performing a linear fit to the t_2 data reveals a power-law scaling $t_2 \propto V^{-1.04 \pm 0.05}$ (black solid line in Figure 3b). The t_1 data, however, are best fitted ($\chi^2 = 1.15$) by an exponential, $t \propto e^{-V/V_0}$ (red solid line in Figure 3b), with $V_0 = 70.5 \pm 3$ mV. Alternatively, a power-law $t_1 \propto V^{-4.06 \pm 0.11}$ (which would be a straight line in Figure 3b) describes the data also well ($\chi^2 = 5.82$).

Finally, at each voltage we analyze the fraction of events that show multiple positive conductance change levels; see the inset of Figure 2b for an example of such event. Multilevel events have previously been associated with DNA that translocates not from head to tail, but in a folded fashion where the DNA bends as it enters the pore.^{14,15} Interestingly, we do observe multiples of ΔG levels for the conductance increases, but we do not observe multiples of the negative of ΔG levels (see for example the histogram in Figure 1f that shows only one peak at negative ΔG but two distinct peaks at positive ΔG). This suggests that the positive ΔG is associated with a translocation process that can involve DNA folding but that the negative ΔG is not. We find that the fraction of these folded events is negligible at low voltages but increases to substantial fractions at higher voltages (Figure 2b).

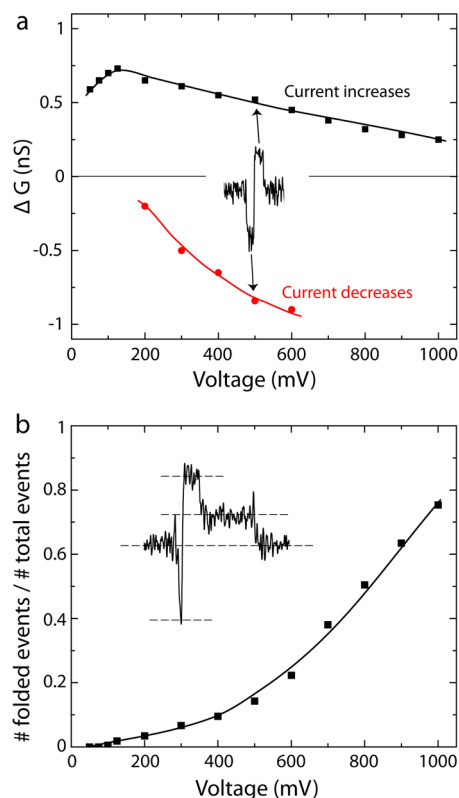


Figure 2. (a) Voltage dependence of the magnitude of the conductance-increase levels (black points), as well as conductance-decrease levels (red points) for λ -DNA translocations at 0.1 M KCl through a 6 nm nanopore. (b) Fraction of folded events as a function of voltage. The inset shows the trace of a folded event taken at 500 mV.

Discussion. How can we understand these striking observations? First, at both low (<200 mV) and high (>600 mV) voltages we exclusively see current increases. This is the expected behavior similar to what was observed in previous work, where current increases were attributed to the flow of counterions along the DNA.¹⁰ However, remarkably, in the regime between 200 and 600 mV we see both current decreases and enhancements within each single event. The values for these boundary voltage ranges are not sharp and can be attributed to our measurement resolution: At low voltages, the magnitude of the current-decrease part of the signal becomes too small to be observed beyond the noise level (Figure 2a), while at high voltages t_1 becomes too short to be measurable within our finite bandwidth (Figure 3).

How can we understand that the current first goes down and then goes up within a single event? Let us first consider the latter, current increase, part of the events. For this part, both the conductance change as a function of voltage, the folding behavior as measured in the multilevel current changes, and the duration of this part of the event, t_2 , are similar to the expected behavior for DNA translocation as reported in many previous reports. In particular, t_2 scales, within errors, as $1/V$, which is characteristic for the translocation of a DNA molecule through the pore. By contrast, however, t_1 is very strongly dependent on voltage, scaling as e^{-V/V_0} , which is not at all what one would expect for unhindered DNA translocation. Furthermore the conductance change for this first current-decrease part of the event sharply increases with voltage. This is similar to previous observations that were attributed to an increased access

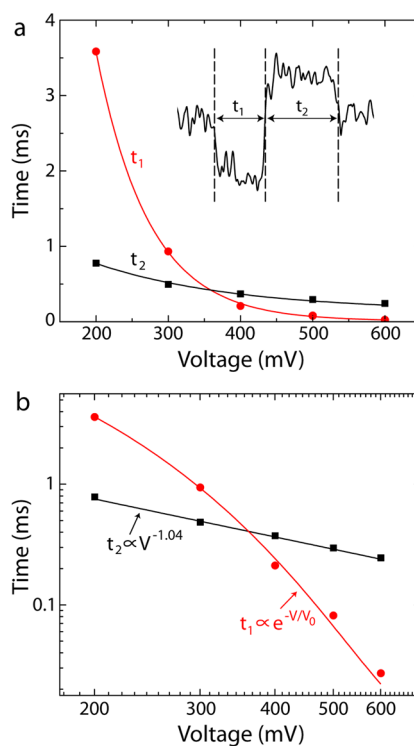


Figure 3. (a) Each multilevel event is divided into its natural two parts, that is, current increase and respectively decrease. We name the duration of the first part t_1 and that of the second part t_2 (example events in the inset). We plot the dependency of t_1 (red circles) and t_2 (black squares) on voltage. We observe that $t_1 > t_2$ below ~ 350 mV, while $t_1 < t_2$ above ~ 350 mV. (b) Same data on a log-log scale. Black solid line is a linear fit, signaling power-law scaling according to: $t_2 \propto V^{-1.04 \pm 0.05}$. Red solid line is an exponential fit to the data: ($t_1 \propto e^{-V/V_0}$), with $V_0 = 70.5$ mV.

resistance (i.e., the resistance of the medium outside the pore) at high voltages for both ssDNA¹⁶ and dsDNA¹⁷ due to the fact that the DNA is pushed closer toward the nanopore entrance at higher voltages.

Combining these observations, we propose the following model to explain the composite events (see also Figure 4): First, the long DNA molecule, which forms a random coil in solution, approaches the nanopore, and enters the access resistance region close to the entrance of the pore. This will decrease the conductance which explains the first part of the observed signal. To pass through the pore, the DNA has two options: (1) it can enter in a folded way, or (2) it changes its configuration so that one of the DNA ends finds the pore entrance after which DNA translocation proceeds in a head-to-tail fashion. Note that given the high stiffness of dsDNA (persistence length of ~ 50 nm, i.e., much larger than the pore diameter) scenario,¹ folded entry, is unlikely for small pores and low voltage bias, as is also supported by our experimental data (Figure 2b). Finally, in a second step of the process, the DNA enters the nanopore, and counterions start to flow along the DNA, leading to a current enhancement which explains the second part of the observed current signal.

Our qualitative physical picture of the process thus is the following. First, the DNA blob (which has a radius of gyration of about 800 nm¹⁸) docks onto the nanopore. This leads to a measurable increase in the access resistance. Next, given that entrance in a folded way is unlikely, one of the DNA ends will have to move from a random location within the DNA coil to

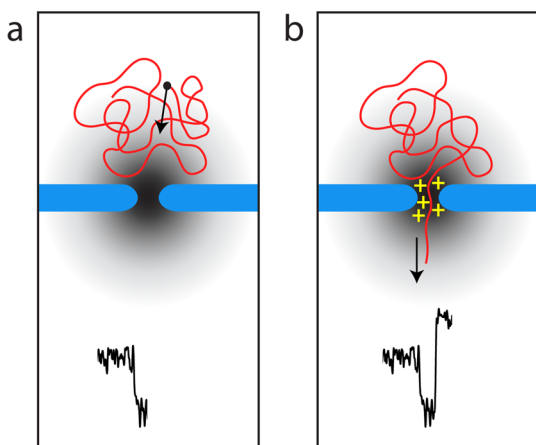


Figure 4. Proposed model describing the hybrid events. (a) First, DNA spends time in the access resistance region, which leads to a current decrease. During this docking time, one of the two DNA ends has to find its way to the nanopore. (b) Subsequently, the DNA enters the pore and translocates, which leads to a current increase due to enhanced flow of counterions along the DNA.

the pore entrance. It is not a priori clear how the search time of a DNA end will scale with voltage. Empirically, we find that this search time is very strongly dependent on voltage ($t \propto e^{-V/V_0}$). Previously, it has been shown that the capture radius—that is, the distance from the nanopore within which a molecule is attracted so strongly by the electric field that it is more likely to enter the nanopore than to diffuse away—scales linearly with voltage.¹⁹ Assuming, for simplicity, that only diffusion plays a role, this would suggest (from the equation for Brownian diffusion, $\langle \Delta x^2 \rangle \geq 2Dt$) a quadratic scaling of capture time with voltage. In our case, however, on top of this, there is also the effect that the DNA ends experience a biased motion due to the voltage gradient, and furthermore the DNA blob will get flattened at higher voltages as it hovers above the nanopore (as is apparent from the strong increase of negative ΔG values with voltage, see Figure 2a). Both of these effects are voltage-dependent, and both will reduce the time that the DNA end has to move to reach the pore entrance at higher voltages. A detailed quantitative model to explain the measured behavior is however lacking at this point, and our novel data present an interesting challenge to theorists.

This picture of a two-phase translocation process adequately explains all our observations. Our model thus indicates that these composite events allow us to independently measure the docking time before translocation (t_1) and the actual translocation time (t_2). Note that a similar process might also take place in larger pores, but in that case t_1 will be shorter, likely immeasurably short. Signatures of events with features similar to those reported in the current work were reported before in experiments²⁰ and simulations,²¹ albeit in pores that were smaller than the 2 nm diameter of the dsDNA molecule. In that case, the physics of the translocation process is much different than for larger nanopores (like those used here) that do provide enough space for the DNA to translocate without strong deformation. Theoretical work on translocation of charged cylinders also predicted hybrid composite events.²² It was speculated^{21,22} that, when DNA rapidly exits the pore, a cloud of ions that accumulated near the pore's entrance is released, resulting in a transient increase of the ionic current above the open pore level. However, this would mean that the first part of the event would be the true translocation, whereas

the second part would be not, and this alternative explanation does not fit our t_1 and t_2 data, neither does it fit the measured voltage dependence of both current levels. Finally, very recently a high-bandwidth setup was realized²³ that led to the measurement of multilevel events, albeit with both levels being current decreases, at high salt. These events were attributed to trapping of the DNA in a sideways orientation on top of a nanopore, followed by translocation, which is related but different from the observation in the current work.

In conclusion, we discovered a new type of hybrid composite events where the current within each event first decreases and subsequently increases. Data analysis shows that these events signal the sequential docking and translocation of a DNA molecule through a nanopore. These findings allow us to independently measure the actual translocation time and the docking time before translocation and show that the contribution of the access resistance to the overall current signature cannot be neglected.

Materials and Methods. Fabrication of solid-state nanopores starts with the fabrication of 20 nm thin free-standing SiN membranes through the use of electron-beam lithography and wet etching.⁸ For the electrical measurements, a membrane with a single nanopore is mounted in a polyether ether ketone (PEEK) microfluidic flow cell and sealed to liquid compartments on either side of the sample. All reported DNA translocation experiments were performed with unmethylated λ -DNA (10 ng/ μ L, Promega), a nanopore that measured 6 nm in diameter in 100 mM KCl, 10 mM Tris-HCl, and 1 mM EDTA at pH 8.0 at room temperature. An current–voltage curve for this nanopore is presented in the Supporting Information; see Figure S1. Ag/AgCl electrodes are used to detect ionic currents and to apply electric fields. The high voltage measurements were performed after the low voltage measurements. Current traces are measured at 100 kHz bandwidth using a resistive feedback amplifier (Axopatch 200B) and digitized at 500 kHz. Additional low-pass filtering at 10 kHz is applied at voltages of 100 mV and below. The event-fitting algorithm used to analyze and label the translocation events was the same as the one described before.¹⁴

■ ASSOCIATED CONTENT

📄 Supporting Information

Measured current–voltage (I – V) characteristics for the 6 nm in diameter nanopore used in this study and an event scatter plot of time duration versus conductance blockade for all events recorded at 500 mV. This material is available free of charge via the Internet at <http://pubs.acs.org>.

■ AUTHOR INFORMATION

✉ Corresponding Author

*E-mail: c.dekker@tudelft.nl

📄 Notes

The authors declare no competing financial interest.

■ ACKNOWLEDGMENTS

We thank M. Muthukumar for discussions. This work is supported by the EC program NanoSci-E+, the European Union's Seventh Framework Program (FP7/2007-2013) under Grant agreement No. 201418 (READNA), and ERC-2009-AdG Grant 247072 NANOforBIO.

■ REFERENCES

- (1) Dekker, C. *Nat. Nanotechnol.* **2007**, *2*, 209.
- (2) Howorka, S.; Siwy, Z. *Chem. Soc. Rev.* **2009**, *38*, 2360.
- (3) Branton, D.; Deamer, D. W.; Marziali, A.; Bayley, H.; Benner, S. A.; Butler, T.; Di Ventra, M.; Garaj, S.; Hibbs, A.; Huang, X.; et al. *Nat. Biotechnol.* **2008**, *26*, 1146.
- (4) Aksimentiev, A. *Nanoscale* **2010**, *2*, 468.
- (5) Venkatesan, B. M.; Bashir, R. *Nat. Nanotechnol.* **2011**, *6*, 615.
- (6) Kowalczyk, S. W.; Blosser, T. R.; Dekker, C. *Trends Biotechnol.* **2011**, *29*, 607.
- (7) Keyser, U. F. J. *R. Soc. Interface* **2011**, *8*, 1369.
- (8) Kowalczyk, S. W.; Hall, A. R.; Dekker, C. *Nano Lett.* **2010**, *10*, 324.
- (9) Schneider, G. F.; Dekker, C. *Nat. Biotechnol.* **2012**, *30*, 326.
- (10) Smeets, R. M.; Keyser, U. F.; Krapf, D.; Wu, M. Y.; Dekker, N. H.; Dekker, C. *Nano Lett.* **2006**, *6*, 89.
- (11) Chang, H.; Kosari, F.; Andreadakis, G.; Alam, M. A.; Vasmatzis, G.; Bashir, R. *Nano Lett.* **2004**, *4*, 1551.
- (12) Fan, R.; Karnik, R.; Yue, M.; Li, D.; Majumdar, A.; Yang, P. *Nano Lett.* **2005**, *5*, 1633.
- (13) Kowalczyk, S. W.; Dekker, C. *Proc. Nanopores Conf. Lanzarote (Roy. Soc. Chem.)* **2012**, in press.
- (14) Storm, A. J.; Storm, C.; Chen, J.; Zandbergen, H.; Joanny, J.-F.; Dekker, C. *Nano Lett.* **2005**, *5*, 1193.
- (15) Li, J.; Gershow, M.; Stein, D.; Brandin, E.; Golovchenko, J. A. *Nat. Mater.* **2003**, *2*, 611.
- (16) Kowalczyk, S. W.; Tuijtel, M. W.; Donkers, S. P.; Dekker, C. *Nano Lett.* **2010**, *10*, 1414.
- (17) Kowalczyk, S. W.; Grosberg, A. Y.; Rabin, Y.; Dekker, C. *Nanotechnology* **2011**, *22*, 315101.
- (18) Schmatko, T.; Bozorgui, B.; Geerts, N.; Frenkel, D.; Eiser, E.; Poon, W. C. K. *Soft Matter* **2007**, *3*, 703.
- (19) Wanunu, M.; Morrison, W.; Rabin, Y.; Grosberg, A. Y.; Meller, A. *Nat. Nanotechnol.* **2010**, *5*, 160.
- (20) Heng, J. B.; Ho, C.; Kim, T.; Timp, R.; Aksimentiev, A.; Grinkova, Y. V.; Sligar, S.; Schulten, K.; Timp, G. *Biophys. J.* **2004**, *87*, 2905.
- (21) Aksimentiev, A.; Heng, J. B.; Timp, G.; Schulten, K. *Biophys. J.* **2004**, *87*, 2086.
- (22) Liu, H.; Qian, S.; Bau, H. H. *Biophys. J.* **2007**, *92*, 1164.
- (23) Rosenstein, J. C.; Wanunu, M.; Merchant, C. A.; Drndic, M.; Shepard, K. L. *Nat. Meth.* **2012**, *9*, 487.